



CHORUS

This is the accepted manuscript made available via CHORUS. The article has been published as:

Efimov–van der Waals universality for ultracold atoms with positive scattering lengths

Paul M. A. Mestrom, Jia Wang, Chris H. Greene, and José P. D'Incao

Phys. Rev. A **95**, 032707 — Published 30 March 2017

DOI: [10.1103/PhysRevA.95.032707](https://doi.org/10.1103/PhysRevA.95.032707)

Efimov-van-der-Waals universality for ultracold atoms with positive scattering lengths

Paul M. A. Mestrom,¹ Jia Wang,² Chris H. Greene,³ and José P. D’Incao^{4,5}

¹*Eindhoven University of Technology, P. O. Box 513, 5600 MB Eindhoven, The Netherlands*

²*Centre for Quantum and Optical Science, Swinburne University of Technology, Melbourne, Australia*

³*Department of Physics and Astronomy, Purdue University, West Lafayette, Indiana 47907, USA*

⁴*JILA, University of Colorado and NIST, Boulder, Colorado 80309, USA*

⁵*Department of Physics, University of Colorado, Boulder, Colorado 80309, USA*

We study the universality of the three-body parameters for systems relevant for ultracold quantum gases with positive s -wave two-body scattering lengths. Our results account for finite-range effects and their universality is tested by changing the number of deeply bound diatomic states supported by our interaction model. We find that the physics controlling the values of the three-body parameters associated with the ground and excited Efimov states is constrained by a variational principle and can be strongly affected by d -wave interactions that prevent both trimer states from merging into the atom-dimer continuum. Our results enable comparisons to current experimental data and they suggest tests of universality for atomic systems with positive scattering lengths.

PACS numbers: 31.15.ac,31.15.xj,67.85.-d

I. INTRODUCTION

The recent theoretical and experimental progress in the exploration of ultracold quantum gases in the strongly interacting regime have largely established the relevance of the three-body Efimov physics [1–3] for the understanding of both dynamics and stability of such systems [4–12]. The control of interatomic interactions through magnetic-field dependent Feshbach resonances [13] allows for dramatic changes in the s -wave two-body scattering length, a , making it possible to tune systems to the vastly different collective (mean-field) regimes of attractive, $a < 0$, and repulsive, $a > 0$ interactions. In the regime of strong interactions, $|a|/r_{\text{vdW}} \gg 1$, where r_{vdW} is the van der Waals length [13], the Efimov effect is manifested through the appearance of an infinite series of three-body states that can lead to scattering resonances and interference effects accessible to experiments [2, 3]. Such dramatic few-body phenomena open up the possibility to explore new quantum regimes in ultracold gases. One of the striking signatures of the Efimov effect is the geometric scaling of the system for many trimer properties, which interrelates all the three-body observables via the geometric factor e^{π/s_0} , where $s_0 \approx 1.00624$ for identical bosons. As a result, if universal scaling holds, the determination of a single observable — the *three-body parameter* — would allow derivation of all properties of the system. However, since the early days of Efimov’s original prediction it was largely accepted that this three-body parameter would be different for every system. Nevertheless, a few years ago, as experiments in ultracold gases evolved, it became clear that this concept needed reassessment.

The turnaround came from the experimental observations in ^{133}Cs [14] showing that the three-body parameter a_- , associated with the value of $a < 0$ at which the first Efimov state merges with the three-body continuum, were the same (within a 15% margin) for different resonances in ^{133}Cs . Moreover, if the results were recast in

terms of r_{vdW} , the observations in every other available atomic species also led to similar results, $a_-/r_{\text{vdW}} \approx -10$ (see Ref. [3] for a summary of such experimental findings). Theoretical works then successfully confirmed and interpreted the universality of the a_- parameter [15–21] and consolidated a new universal picture for Efimov physics in atomic systems dominated by van der Waals forces.

This paper assesses the universality of the three-body parameter in the yet unexplored regime of positive scattering lengths, $a > 0$. The available experimental data for Efimov features within this regime is relatively sparse and, consequently, does not clearly display the same degree of universality found for $a < 0$. Although not explicitly demonstrated here, our present theoretical study shows that universality for $a > 0$ persists and is rooted in the same suppression of the probability of finding particles at short distances previously found for $a < 0$ [15–17]. The observables we analyze are related to the value of a at which an Efimov state intersects the atom-dimer threshold, a_* , thus causing a resonance in atom-dimer collisions [22, 23], and the value a_+ at which a minimum in three-body recombination occurs as a result of a destructive interference between the relevant collision pathways [22, 24–26]. One important feature that can help to interpret our computed values for a_* and a_+ associated with the ground Efimov state is the existence of a variational principle [27, 28] that constrains its energy to always lie below a certain value lower than the dimer energy, thus preventing the trimer to cross the atom-dimer threshold. This has a direct impact on both the lowest atom-dimer resonance and on interference phenomena, even when, as we show here, the conditions for the validity of that variational principle are not strictly satisfied. Moreover, our analysis indicates that the presence of strong d -wave interactions [29, 30], and/or possibly some other finite-range effects, also prevents the first excited Efimov state from merging with the dimer threshold, although it still produces a resonance feature in atom-dimer observables

and a recombination minimum for small a .

II. BRIEF THEORETICAL BACKGROUND

Here we use the adiabatic hyperspherical representation which offers a simple and conceptually clear description of few-body systems while still accurately determining their properties [3]. Within this representation, after solving for the hyperangular internal motion—which includes all interparticle interactions—three-body observables can be obtained by solving the hyper-radial Schrödinger equation [31]

$$\left[-\frac{\hbar^2}{2\mu} \frac{d^2}{dR^2} + W_\nu \right] F_\nu(R) + \sum_{\nu' \neq \nu} W_{\nu\nu'}(R) F_{\nu'}(R) = E F_\nu(R). \quad (1)$$

where the hyperradius R describes the overall size of the system, $\mu = m/\sqrt{3}$ is the three-body reduced mass and ν is an index including all necessary quantum numbers to characterize each channel. Equation (1) describes the radial motion governed by the effective hyperspherical potentials W_ν and non-adiabatic couplings $W_{\nu\nu'}$, which determine all bound and scattering properties of the system. In the present study, each pair of particles interacts via a Lennard-Jones potential

$$v_{LJ}(r) = -\frac{C_6}{r^6} \left(1 - \frac{\lambda^6}{r^6} \right), \quad (2)$$

where λ is adjusted to give the desired value of a and C_6 is the usual dispersion coefficient. Note that our calculations use van der Waals units (with energy and length units of $E_{\text{vdW}} = \hbar^2/mr_{\text{vdW}}^2$ and r_{vdW}) such that the specification of the value of C_6 is unnecessary. Our present study is centered around the first three poles of a , which occur at the values denoted $\lambda = \lambda_1^*$, λ_2^* and λ_3^* . One important point to keep in mind is that near λ_1^* there can exist only a single two-body s -wave state, whereas near λ_2^* and λ_3^* multiple deeply bound states exist (4 and 9, respectively), owing to the presence of higher partial wave dimers.

III. RESULTS

Figure 1 shows the energies of the lowest three Efimov states, E_{3b} , for values of a near the three poles considered (λ_1^* , λ_2^* and λ_3^*), offering a global view of the degree of the universality of our results. Near λ_1^* , Efimov states (black filled circles) are true bound states while near λ_2^* and λ_3^* (red and green open circles, respectively) Efimov states are resonant states whose (presumably nonuniversal) widths have been calculated using the Ref. [32] procedure, indicated in Fig. 1 as the error bars. The atom-dimer threshold, defined by the dimer

energy, $E_{2b} = -\hbar^2/ma^2$ ($a \gg r_{\text{vdW}}$), is also shown (solid line). In Fig. 1 the ground Efimov state does not “cross”

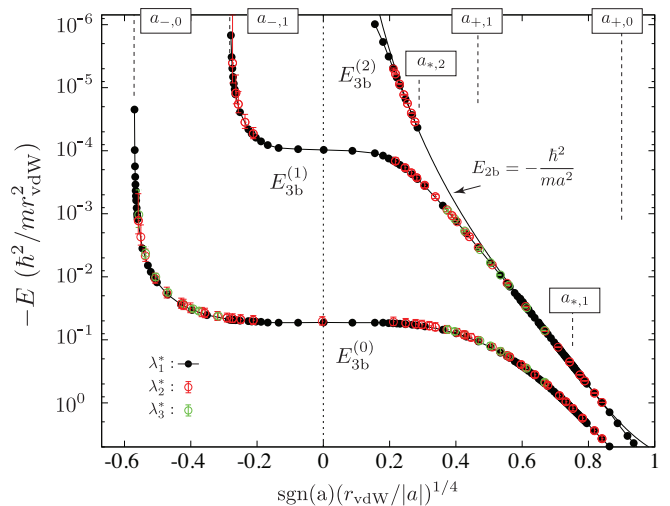


FIG. 1: Energy of Efimov states calculated near the first three poles of a , $\lambda = \lambda_1^*$, λ_2^* and λ_3^* , in our model potential in Eq. (2). Near λ_1^* , Efimov states (black filled circles) are true bound states while near the λ_2^* and λ_3^* (red and green open circles, respectively) Efimov states are resonant states with the corresponding widths indicated as the error bars. Approximated values for a_- , a_* , and a_+ are also indicated.

or intersect the atom-dimer threshold, as expected from the variational principle in Refs. [27, 28], which state that $E_{3b} < 3E_{2b}$. In principle, this variational constraint applies only to bound states, i.e., only for Efimov states near λ_1^* , however, our calculations for the energies of Efimov resonances near λ_2^* and λ_3^* also follow the same non-crossing rule. Evidently, this effect strongly modifies the expected universality predicted by zero-range models since it prevents an atom-dimer resonance and can also modify the minima in recombination associated with the ground Efimov state. Table I summarizes our computed values of the three-body parameters—see also Fig. 1 for their approximate location. [The values for a_- were previously determined in Ref. [15] (and in unpublished work from that study).] The additional index on the a_- , a_+ , and a_* parameters indicates their Efimov family parentage. The physics involved and caveats on the determination of these three-body parameters are given below.

Closer inspection of Fig. 1 reveals that the first excited Efimov state also fails to intersect with the dimer threshold. This is clearly shown in Fig. 2 for the binding energy of the Efimov states, $E_b = E_{2b} - E_{3b}$. Near λ_1^* (black filled circles) the non-crossing of the first excited state is evident within the shaded region in Fig. 2. Near λ_2^* (red open circles), the qualitative behavior is the same, however: As the energy of the Efimov state approaches the threshold its width increases to the point in which it exceeds the value of its binding energy—therefore, losing some its “bound” state character—and eventually “dissolving” into the atom-dimer continuum (see shaded

TABLE I: Values for the three-body parameters a_- , a_* and a_+ for the lowest two Efimov scattering features in recombination and atom-dimer collisions, near the lowest three poles in the scattering length. For $a_{+,1}$ we also show its dependence on the temperature by $\langle K_3 \rangle$ (see text) at values of $k_B T/E_{\text{vdW}}$ (indicated in square brackets) listed in the last three columns below. In the bottom part of the table we list the universal ratios $\theta_{ij}^{\alpha\beta}$ [see Eq. (3)] resulting from the average value of the three-body parameters (see text for the comparison with the zero-range results).

	$a_{-,i}/r_{\text{vdW}}$	$a_{*,i}/r_{\text{vdW}}$	$a_{+,i}/r_{\text{vdW}}$	$\langle a_{+,1} \rangle / r_{\text{vdW}}$		
Pole	$(i=0,1)$	$(i=1,2)$	$(i=0,1)$	$[10^{-4}]$	$[3 \times 10^{-4}]$	$[10^{-3}]$
λ_1^*	-9.60, -161	3.41, 157	1.41, 27.2	28.0	29.1	32.1
λ_2^*	-9.74, -164	3.26, 160	1.41, 27.9	28.7	30.7	34.8
λ_3^*	-9.96, —	3.33, 160	1.41, 28.0	—	—	—
Avg.	-9.77, -163	3.33, 159	1.41, 27.7	28.4	29.9	33.5
(i,j)	(0,0)	(0,1)	(1,0)	(1,1)	(2,0)	(2,1)
θ_{ij}^{+-}	0.143	0.195	0.125	0.170	—	—
θ_{ij}^{*-}	—	—	0.015	0.020	0.032	0.043
θ_{ij}^{*+}	—	—	0.105	0.120	0.220	0.253

region in Fig. 2). Passing this point, as a decreases further, the state recovers its bound character. Our physical interpretation of the non-crossing of the first excited Efimov state [33] is that it results from the existence of strong d -wave interactions near $a/r_{\text{vdW}} = 1$ [29, 30]. Within our theoretical model, since s - and d -wave interactions can not be separated, a more clear physical picture of the non-crossing of the first excited Efimov state still remains, leaving even the possibility of that being a generalization of the same variational principle [27, 28] which prevents the ground state to unbind. Figure 2 shows that only the second excited Efimov state displays the expected intersection with the atom-dimer threshold.

Evidently, the effects analyzed above have an important impact on the determination of the three-body parameter a_* . This is achieved here by directly calculating the corresponding atom-dimer scattering properties. Of particular importance for ultracold experiments is the atom-dimer scattering length a_{ad} and the atom-dimer loss rate β [34]. Figure 3 shows our calculated values for these quantities. In Fig. 3 (a), around the shaded region (corresponding to the same shaded region in Fig. 2) a_{ad} is enhanced, however, remaining always positive and consistent with the failure of the first excited Efimov state in Fig. 2 to become unbound. (Note that in this regime a_{ad} for λ_2^* and λ_3^* displays a more complicated dependence on a due to the presence of strong couplings to nearby three-body channels.) For larger a , a_{ad} is now enhanced and changes sign, implying that the second excited Efimov state intersects with the dimer energy (see Fig. 2). Note that here, a_{ad} for λ_2^* and λ_3^* does not actually diverge due to the presence of inelastic processes [35]. Figure 3(b)

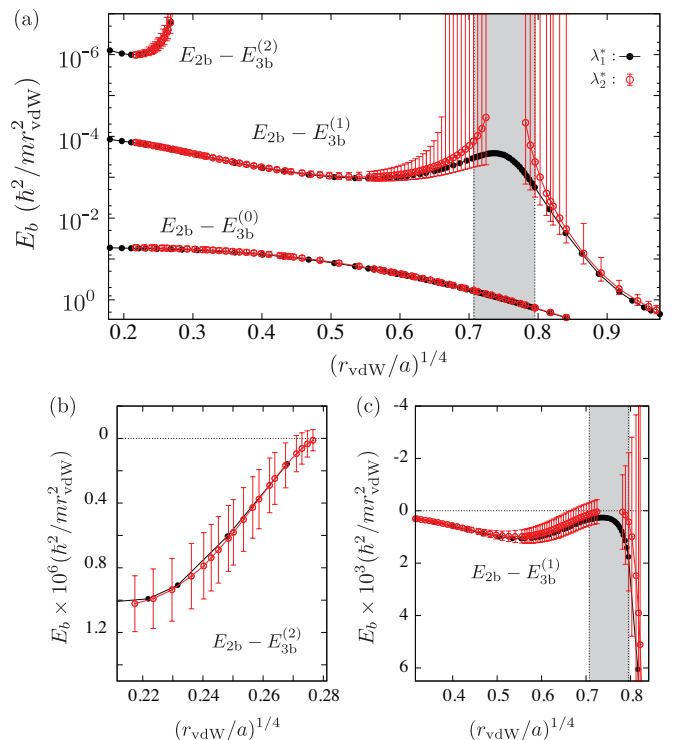


FIG. 2: (a) Binding energies, $E_b = E_{2b} - E_{3b}$, of Efimov states near λ_1^* and λ_2^* (black filled and red open circles, respectively) showing that both ground and first excited Efimov states fail to merge into the atom-dimer threshold (see text). In (b) and (c) we show a blow up of (a) near the second and first excited Efimov states, respectively.

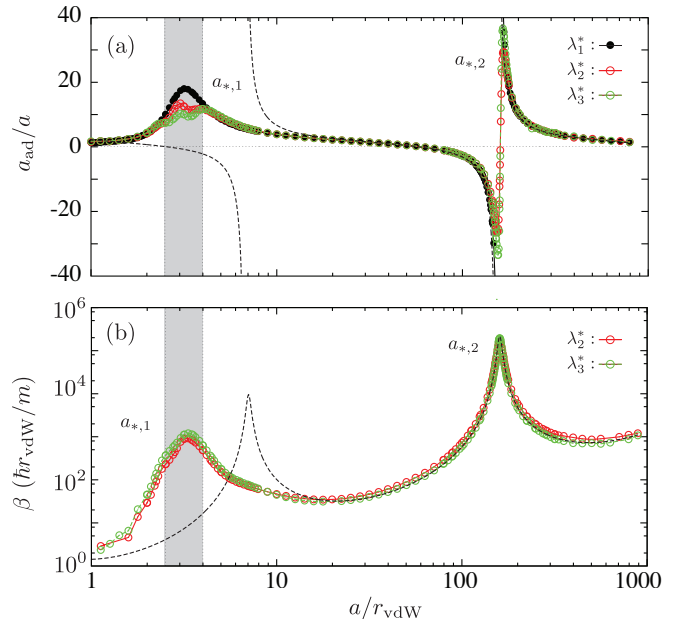


FIG. 3: (a) The atom-dimer scattering length, a_{ad} , and (b) corresponding loss rate, β , displaying resonant behavior due to Efimov resonances associated with the first and second excited Efimov states. The values of the three-body parameters $a_{*,1}$ and $a_{*,2}$ are indicated in the figure. The dashed curve gives the analytical zero range results from Ref. [23].

shows the corresponding atom-dimer loss rates, which display the resonant behavior associated with the first and second excited Efimov states. Even though the first excited Efimov state does not become unbound, it approaches the atom-dimer threshold close enough to produce a clear enhancement in the atom-dimer loss rate. We define $a_{*,1}$ and $a_{*,2}$ as the value of a where β is maximum [see Fig. 3 (b)], except for our calculations near the first pole, where no losses occur ($\beta = 0$). In this case $a_{*,1}$ and $a_{*,2}$ were determined from the maximum value of a_{ad} [see Fig. 3(a)]. Numerical values are listed in Table I. In order to contrast our numerical results with the universal predictions (based on two-body contact interaction models), we also display in Fig. 3 (dashed lines) the expected behavior for a_{ad} and β from Ref. [23]. For the zero-range, universal, model of Ref. [23] we used the averaged value for $a_{*,2}$ from Table I as the three-body parameter, and set the inelasticity parameter $\eta = 0$ in Fig. 3(a) and $\eta = 0.03$ for Fig. 3(b), in order to better fit the data for λ_3^* . Although the agreement is very good for large a , near $a_{*,1}$ not only finite range corrections become more important but also the fact that the first excited Efimov state fails to intersect with the atom-dimer threshold, imply strong deviations between universal zero-range theory and our results.

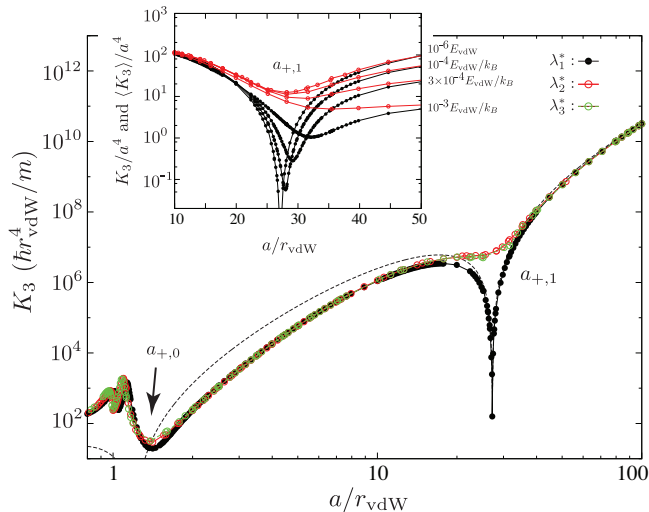


FIG. 4: Three-body recombination, K_3 , displaying interference minima associated with the ground and first excited Efimov states. Values of the three-body parameters $a_{+,0}$ and $a_{+,1}$ are indicated in the figure. The dashed curve gives the analytical zero range result in the absence of deeply bound dimers [2, 38]. *Inset*: Thermally averaged recombination rate, $\langle K_3 \rangle$, illustrating the temperature dependence of $\langle a_{+,1} \rangle$.

Finally, we have also calculated the three-body recombination rate, K_3 , in the lowest three-body angular momentum ($J = 0$) [36, 37] to determine the values of the three-body parameter a_+ . Figure 4 shows our results for K_3 in the zero-energy limit ($E = 10^{-6} E_{\text{vdW}}$) clearly displaying two minima, whose locations are identified as the values for $a_{+,0}$ and $a_{+,1}$ listed in Table I. Our numerical

results obtained near λ_1^* are compared with the analytical results in the absence of deeply bound dimers [2, 38] (dashed line). For large a our results agree well with the analytical ones while strong deviations can be observed for small a . In particular, one can see that the predicted minimum in recombination near $a/r_{\text{vdW}} = 1$ is strongly affected by finite-range effects. We trace such effects to the presence of strong d -wave interactions [33]. In fact, near $a/r_{\text{vdW}} = 1$ our results display an enhancement due to a universal three-body resonance with strong d -wave character [30]. Therefore, our result for $a_{+,0}$ is a balance between universal s - and d -wave physics [33]. The inset of Fig. 4 shows the temperature dependence of K_3 obtained by calculating the thermally averaged recombination rate $\langle K_3 \rangle$ [37], which illustrates the temperature dependence of $\langle a_{+,1} \rangle$ in the regime relevant for experiments —see also the values listed in Table I. In principle, at finite temperatures one would also need to include higher partial-waves contributions to recombination. For identical bosons, however, the next leading contribution is for $J = 2$ and scale with the temperature and scattering length as $T^2 a^8$ [37]. In that case, for the temperatures we explore in Fig. 4 and values for $\langle a_{+,1} \rangle$ listed Table I, such effects are likely to be small, except perhaps for our largest temperature, where $ka_{+,1} \approx 0.88$ (see also the analysis in Ref. [37]).

Our results for the three-body parameters — summarized in Table I— clearly show universal behavior (with deviations between themselves within a few percent) and should be applied for atomic species with isolated broad Feshbach resonances. We also used our results in Table I to determine other universal properties —for instance, the ratios a_+/a_- , a_*/a_- , and a_*/a_+ — and compare with those resulting from zero-range models [2, 39]. For that we define the ratio between different three-body parameters as

$$a_{\alpha,i}/a_{\beta,j} = \theta_{ij}^{\alpha\beta} (e^{\pi/s_0})^{i-j}, \quad (3)$$

where α and β can assume the values “−”, “+” and “*”, while i and j run over the index labeling the Efimov state. Within the zero-range model θ is a universal number and does not depend on i and j : $\theta_{ij}^{+-} \approx 0.210$; $\theta_{ij}^{*-} \approx 0.047$; $\theta_{ij}^{*+} \approx 0.224$ [2, 39]. Comparing those with the ones shown in the bottom part of Table I (calculated using the averaged values for a_- , a_+ and a^*) we have found substantial deviations, most likely due to finite-range effects and the absence of d -wave interactions in the zero-range model. Moreover, the values for the geometric scaling factors obtained from our calculations, $a_{-,1}/a_{-,0} \approx 16.7$, $a_{+,1}/a_{+,0} \approx 19.7$, and $a_{*,2}/a_{*,1} \approx 47.8$, also display strong deviations from the universal value $e^{\pi/s_0} \approx 22.69$. We note that the results for the geometric scaling factor for a_- obtained in Refs. [18, 40] are consistent to ours but the corresponding results for a_* from [18] are not. A comparison with results originated from models which include finite-range corrections [18, 40–44] needs to be made carefully to ensure that the interaction parameters

are the same. This, however, is beyond the scope of the present study. A more direct comparison, however, can be made with the work in Ref. [45], where a model similar to ours, however, considering only s -wave interactions, is used. The calculations of Ref. [45] involve a separable approximation of a hard-core-type van der Waals potential as two-body interaction potential. The comparison between our results and the ones from Ref. [45] thus provides a sense of how important d -wave interactions might be. In Table II we list our average results, marked by LJ, (see Table I) and the corresponding average results from Ref. [45], marked by LJ^s. In Table II we also list the value of $\kappa_0 = (mE_{3b}^{(0)}/\hbar^2)^{1/2}$ obtained from our calculations for λ_1^* and the corresponding averaged result from Ref. [45]. The agreement is generally good for all cases (the relative differences are indicated in Table II between square brackets), with the exception for the value of $a_{*,1}$, most likely because the non-crossing of the first excited Efimov state is absent in the model of Ref. [45], clearly indicating a strong effect due to d -wave interactions. We note, however, that the agreement for the geometric factors $a_{-,1}/a_{-,0}$ and $a_{+,1}/a_{+,0}$ are generally better than the absolute values of the three-body parameters. This indicates that the effect of the d -wave interactions in such parameters is mainly to introduce a shift:

$$a_x \rightarrow a_x e^{-\phi_d/s_0}, \quad (4)$$

or, equivalently, a change in the three-body phase: $s_0 \ln(a/a_x) \rightarrow s_0 \ln(a/a_x) + \phi_d$. Indeed, forcing our value of $a_{+,0}$ to reproduce the one from Ref. [45], we obtain $\phi_d \approx -0.146$ and the resulting rescaled three-body parameters, marked by LJ* in Table II now agree much better, evidently, with the exception of $a_{*,1}$. The above rescaling process, therefore, can be seen as an attempt to subtract-off d -wave effects from our calculations, although a more rigorous study that can provide a more quantitative analysis of such effects still needs to be performed.

TABLE II: Comparison between the average results for the three-body parameters in Table I, marked here by LJ, and the corresponding average results from Ref. [45], marked by LJ^s. The Table also lists the value of $\kappa_0 = (mE_{3b}^{(0)}/\hbar^2)^{1/2}$ obtained from our calculations for λ_1^* and the corresponding averaged result from Ref. [45]. The corresponding relative differences between the LJ-LJ^s and LJ-LJ* models are indicated between square brackets.

	$a_{-,i}$ ($i = 0, 1$)	$a_{-,1}/a_{-,0}$	κ_0	$a_{+,i}$ ($i = 0, 1$)	$a_{+,1}/a_{+,0}$	$a_{*,1}$
LJ	-9.77,-163	16.7	0.230	1.41,27.7	19.7	3.33
LJ ^s	-10.7,-187 [0.10,0.15]	17.5 [0.05]	0.193 [0.16]	1.63,33.5 [0.16,0.21]	20.6 [0.05]	5.49 [0.65]
LJ*	-11.3,-188 [0.05,0.01]	16.7 [0.05]	0.199 [0.03]	1.63,32.0 [0.00,0.05]	19.7 [0.05]	3.85 [0.43]

TABLE III: Experimental values for the three-body parameters a_+ and a_* . The table displays our assignment of the parameters by indicating the value of i for $a_{+,i}$ and $a_{*,i}$ for each case. We also list the values for a/a_c [37] characterizing the degree of thermal effects in the experimental data.

Atom	a_+/a_c	i	$a_{+,i}/r_{vdW}$	a_*/a_c	i	$a_{*,i}/r_{vdW}$
¹³³ Cs	0.08	0	2.1(0.1) [46]	0.13	1	4.2(0.1) [54, 55]
	0.03	0	2.7(0.3)[14]	0.24	1	6.5(0.3) [55]
	—	0	2.5(0.4) [47]			
⁷ Li	0.02	0	2.7(0.1)[48, 49]	0.09	1	13.0(0.6) [48, 49] [†]
	0.29	1	44(3) [48, 49]	0.04	1	5.5 [56]
	0.32	1	35(4) [50, 51]	0.05	1	6.0(0.1) [56] [†]
³⁹ K	0.34	1	39(2) [51, 52]			
	0.03	0	3.5(0.1) [53]	0.01	0	0.5(0.2) [53] [†]
	0.76	1	88(14) [53]	0.12	1	14.4(0.6) [53] [†]
⁶ Li				0.01	1	2.9 [57]

We now analyze the currently available experimental data for a_+ and a_* listed (and assigned) in Table III. As one can see from Table III, the values listed for $a_{+,0}$ and $a_{+,1}$ are qualitatively consistent among themselves, with the exception of the data for ³⁹K [53] — a new analysis presented in Ref. [58] suggests that this data might be subject of a new calibration. Although the values for $a_{+,1}$ in Table III are likely to suffer from thermal effects (the condition $|a| \ll a_c = \hbar/\sqrt{mk_B T}$ [37] ensuring the absence of thermal effects is not strictly satisfied), our finite temperature calculations covering the range of temperatures relevant for the experiments (see Table I) indicate that thermal effects might lead to no more than a 10% variation from the zero temperature result. We also note that for ⁷Li and ³⁹K the resonances are substantially less broad than the ones for ¹³³Cs (see Ref. [13]), thus opening up the possibility of finite-width effects as responsible for the deviations among the experimental data in Table III. In comparison to the values for a_+ , the results for $a_{*,1}$ listed in Table III display a much stronger deviation among themselves. A more careful analysis, therefore, is necessary in order to understand some of the possible factors affecting such observations. For instance, the value for $a_{*,1}$ for ¹³³Cs from Ref. [55], as well as the results for ⁷Li from Ref. [56], were obtained using a Feshbach resonance that is not well separated from another nearby resonance, possibly affecting the observed value for $a_{*,1}$. Most of the results marked in Table III by “[†]” present the largest variations compared with the total averaged result for $a_{*,1}$ ($\approx 6.63r_{vdW}$). They were, however, obtained based on the assumption that atom-dimer resonances can be observed in atomic samples by means of an avalanche mechanism [53]. Although modifications on the description of such mechanism can lead to more reasonable results [56, 59], this hypothesis is currently considered questionable [55, 60, 61].

Therefore, accordingly to our analysis above, in order to properly compare the experimental data to theoretical

predictions, we excluded the data from ^{39}K [53] and those marked by “†” in Table III. From the remaining experimental data, we determine an average value and corresponding average error as listed in Table IV (the average errors are indicated in parenthesis). Using the zero-range (ZR) universal relations derived in Refs. [2, 39] [Eq. (3)] we determined the values for $a_{+,0}$, $a_{+,1}$ and $a_{*,1}$, using the average value for $a_{-,0}$ in Table I, and list these in Table IV, along with our corresponding averaged results (LJ) from Table I. As one can see, the zero-range results for $a_{+,0}$ and $a_{+,1}$ perform better than our results when compared to the experimental data, while our result for $a_{*,1}$ outperforms the zero-range result. In fact, within the zero-range model the atom-dimer resonance associated to $a_{*,1}$ originates from an actual crossing between the first excited Efimov state while in our model it does not (see Fig. 2 and corresponding discussion in the text). We note, however, that our result for $a_{+,1}/a_{+,0}$ better reproduces the value from the experimental data. This indicates that a shift on the position of the three-body parameters for $a > 0$, in the same spirit than the one obtained from Eq. (4), can improve the comparisons of the individual three-body parameters while keeping their ratios unchanged. In fact, as shown in Table IV, using the results for LJ* listed in Table II —obtained via the rescaling in Eq. (4) in order to subtract off d -wave interactions— an overall improved comparison to the experimental data can be observed (see Table IV). Although there is no clear reason why such scaling should be allowed, the above analysis clearly indicates that our numerical results might generate different finite-range effects from the ones in the experimental systems, whether originated from the strong s - and d -wave mixing in our theoretical model or from the finite-width character produced by real interatomic interactions.

TABLE IV: Comparison between the values for the three-body parameters from different theories and the average experimental data, marked by Exp (see text), with average errors indicated in parenthesis. The zero-range (ZR) results were obtained from the universal relations derived in Refs. [2, 39] [Eq. (3)] using the average value for $a_{-,0}$ in Table I while our average results (LJ and LJ*) are those from Table II. The corresponding relative differences between the different theoretical models and the averaged experimental data are indicated between square brackets.

	$a_{+,0}/r_{\text{vdW}}$	$a_{+,1}/r_{\text{vdW}}$	$a_{+,1}/a_{+,0}$	$a_{*,1}/r_{\text{vdW}}$
Exp	2.50(0.10)	39.3(0.12)	15.7(0.22)	4.78(0.20)
ZR	2.05[0.22]	46.5[0.16]	22.7[0.31]	10.4[0.54]
LJ	1.41[0.77]	27.7[0.42]	19.7[0.20]	3.33[0.43]
LJ*	1.63[0.53]	32.0[0.23]	19.7[0.20]	3.85[0.24]

Evidently, there is much to be understood on the effects that realistic interactions can impose in the determination of the three-body parameters. In more realistic systems the short-range multichannel nature of the interactions can produce, for instance, a different mix-

ing of s - and d -wave components than the single channel model does. One can expect d -wave interactions to be more important when the system possesses a small background scattering length, i.e., of the order of r_{vdW} , since in this case the entrance channel physics, obeying the universality of the van der Waals interactions [29], can include a weakly bound d -wave state. Finite-width effects can lead to values of the effective range different than the one produced in our model, also determined by the universal van der Waals physics [62]. Such effects, although not entirely understood yet, can also lead to substantial deviations of the three-body parameters [18]. In fact, the model developed in Ref. [63], which incorporates some of the multichannel physics of the problem, shows a much better agreement between theory and experiment [55], including for the $a < 0$ geometric scaling $a_{-,1}/a_{-,0} \approx 21.0$ from Ref. [64], indicating that both s - and d -wave mixing and finite-width effects might be at the heart of deviations of the three-body parameters for $a > 0$ here obtained, as well as the deviations among the currently available experimental data (Table III). A fundamental difference between the physics for $a < 0$ (where a more robust universal picture was found [15–21] —see Refs. [3, 47] for a summary of such experimental findings) and for $a > 0$ is that corrections for the energy of the weakly bound s -wave dimer, whether originated from mixing of s - and d -wave interactions or finite-width effects, should already lead to modifications on the $a > 0$ three-body parameters. For a_+ , the atom-dimer channel controls the interference effects in recombination via the exit channel while it represents the initial collision channel responsible for the resonant effects determining a_* . In fact, under this perspective, a simple criteria can be established to determine whether s - and d -wave mixing and finite-width effects are important: if the degree of deviation between the binding energy obtained from multichannel interactions and the one obtained from single channel models are substantially different, such effects are likely to be important.

IV. SUMMARY

In conclusion, our present study establishes the universal values for the three-body parameters a_* and a_+ , both relevant for ultracold quantum gases with positive scattering lengths. One of the most interesting results that has emerged from this study is the fact that the first excited Efimov resonance fails to intersect the dimer threshold, which is a surprising difference from the zero-range universal theories that always predict such an intersection. Our interpretation, that this failure of the resonance to intersect the threshold derives from important d -wave interactions, is consistent with findings from another recent study of this $a > 0$ region [65] which uses a nonlocal potential model having no d -wave physics, and which *does* show such an intersection. The robustness of the present prediction thus hinges critically on whether

the d -wave two-body physics is tightly constrained in the way predicted by van der Waals physics in single channel potential models [29, 30]. Whether it is reasonable to expect that in the case of broad two-body Fano-Feshbach resonances, this linkage of two-body s -wave and d -wave resonance positions is satisfied, remains an open question deserving further investigation. However, especially in the case of narrow two-body resonances, s -wave and d -wave resonances are likely to be largely uncorrelated which presumably invalidates the present predictions in the vicinity of $a/r_{\text{vdW}} \approx 1$. Nevertheless, the qualitative agreement between our results and the currently available experimental data partially confirms the notion of universality of Efimov physics for ultracold atoms. However, more experimental data and more sophisticated the-

oretical models incorporating the multichannel nature of the atomic interactions might be necessary in order to quantitatively address present discrepancies.

Acknowledgments

This work was supported in part by the U.S. National Science Foundation (NSF) Grants PHY-1607204 and PHY-1607180 and by the National Aeronautics and Space Administration (NASA). PMAM also acknowledges JILA for the hospitality during his stay. The authors acknowledge S. Kokkelmans and P. Giannakeas for fruitful discussions.

-
- [1] V. Efimov, *Yad. Fiz.* **12**, 1080 (1970); *Sov. J. Nucl. Phys.* **12**, 589 (1971).
- [2] E. Braaten and H.-W. Hammer, *Phys. Rep.* **428**, 259 (2006).
- [3] Y. Wang, J. P. D’Incao, and B. D. Esry, *Adv. At. Mol. Opt. Phys.* **62**, 1 (2013).
- [4] R. J. Fletcher, A. L. Gaunt, N. Navon, R. P. Smith, and Z. Hadzibabic, *Phys. Rev. Lett.* **111**, 125303 (2013).
- [5] B. S. Rem, A. T. Grier, I. Ferrier-Barbut, U. Eismann, T. Langen, N. Navon, L. Khaykovich, F. Werner, D. S. Petrov, F. Chevy, and C. Salomon, *Phys. Rev. Lett.* **110**, 163202 (2013).
- [6] P. Makotyn, C. E. Klauss, D. L. Goldberger, E. A. Cornell, and D. S. Jin, *Nat. Phys.* **10**, 116 (2014).
- [7] R. J. Fletcher, R. Lopes, J. Man, N. Navon, R. P. Smith, M. W. Zwierlein, and Z. Hadzibabic, *arXiv:1608.04377* (2016).
- [8] A. G. Sykes, J. P. Corson, J. P. D’Incao, A. P. Koller, C. H. Greene, A. M. Rey, K. R. A. Hazzard, and J. L. Bohn *Phys. Rev. A* **89**, 021601(R) (2014).
- [9] S. Laurent, X. Leyronas, and F. Chevy, *Phys. Rev. Lett.* **113**, 220601 (2014).
- [10] D. H. Smith, E. Braaten, D. Kang, and L. Platter, *Phys. Rev. Lett.* **112**, 110402 (2014).
- [11] S. Piatecki and W. Krauth, *Nat. Comm.* **5**, 3503 (2014).
- [12] M. Barth and J. Hofmann, *Phys. Rev. A* **92**, 062716 (2015).
- [13] C. Chin, R. Grimm, P. S. Julienne, and E. Tiesinga, *Rev. Mod. Phys.* **82**, 1225 (2010).
- [14] M. Berninger, A. Zenesini, B. Huang, W. Harm, H.-C. Nägerl, F. Ferlaino, R. Grimm, P. S. Julienne, and J. M. Hutson, *Phys. Rev. Lett.* **107**, 120401 (2011).
- [15] J. Wang, J. P. D’Incao, B. D. Esry, and C. H. Greene, *Phys. Rev. Lett.* **108**, 263001 (2012).
- [16] J. P. D’Incao, J. Wang, B. D. Esry, and C. H. Greene, *Few-Body Systems* **54**, 1523 (2013).
- [17] Y. Wang, J. Wang, J. P. D’Incao, and C. H. Greene, *Phys. Rev. Lett.* **109**, 243201 (2012); *ibid.* **115**, 069901 (2015).
- [18] R. Schmidt, S.P. Rath, and W. Zwerger, *Eur. Phys. J. B* **85**, 386 (2012).
- [19] P. Naidon, S. Endo, and M. Ueda, *Phys. Rev. A* **90**, 022106 (2014).
- [20] P. Naidon, S. Endo, and M. Ueda, *Phys. Rev. Lett.* **112**, 105301 (2014).
- [21] D. Blume, *Few-Body Syst.* **56**, 859 (2015).
- [22] J. P. D’Incao and B. D. Esry, *Phys. Rev. Lett.* **94**, 213201 (2005).
- [23] E. Braaten and H.-W. Hammer, *Phys. Rev. A* **75**, 052710 (2007).
- [24] E. Nielsen and J. H. Macek, *Phys. Rev. Lett.* **83**, 1566 (1999).
- [25] B. D. Esry, C. H. Greene, and J. P. Burke, *Phys. Rev. Lett.* **83**, 1751 (1999).
- [26] P. F. Bedaque, Eric Braaten, and H.-W. Hammer, *Phys. Rev. Lett.* **85**, 908 (2000).
- [27] L. W. Bruch and K. Sawada, *Phys. Rev. Lett.* **30**, 25 (1973).
- [28] M. D. Lee, T. Köhler, and P. S. Julienne, *Phys. Rev. A* **76**, 012720 (2007).
- [29] Bo Gao, *Phys. Rev. A* **62**, 050702(R) (2000).
- [30] J. Wang, J. P. D’Incao, Y. Wang, and C. H. Greene, *Phys. Rev. A* **86**, 062511 (2012).
- [31] J. Wang, J. P. D’Incao, and C. H. Greene, *Phys. Rev. A* **84**, 052721 (2011).
- [32] E. Nielsen, H. Suno, and B. D. Esry, *Phys. Rev. A* **66**, 012705 (2002).
- [33] Based on the analysis of the hyperspherical adiabatic potentials we can trace a strong coupling between the relevant s -wave channel for Efimov physics and the d -wave channel associated with the d -wave dimer state, supporting a universal three-body state [30]
- [34] J. P. D’Incao, B. D. Esry, and C. H. Greene, *Phys. Rev. A* **77**, 052709 (2008).
- [35] J. M. Hutson, *New J. Phys.* **9**, 152 (2007).
- [36] H. Suno, B. D. Esry, C. H. Greene, and J. P. Burke, *Phys. Rev. A* **65**, 042725 (2002).
- [37] J. P. D’Incao, H. Suno, and B. D. Esry, *Phys. Rev. Lett.* **93**, 123201 (2004).
- [38] The results from Ref. [2] were multiplied by a factor $3\sqrt{3}$ in order to ensure the proper comparison.
- [39] A. O. Gogolin, C. Mora, and R. Egger, *Phys. Rev. Lett.* **100**, 140404 (2008).
- [40] A. Deltuva, *Phys. Rev. A* **85**, 012708 (2012).
- [41] A. Kievsky and M. Gattobigio, *Phys. Rev. A* **87**, 052719 (2013).

- [42] C. Ji, D. R. Phillips, and L. Platter, *Ann. Phys. (NY)* **327**, 1803 (2012).
- [43] L. Platter, C. Ji, and D. R. Phillips, *Phys. Rev. A* **79**, 022702 (2009).
- [44] C. Ji, E. Braaten, D. R. Phillips, and L. Platter, *Phys. Rev. A* **92**, 030702(R) (2015).
- [45] J.-L. Li, X.-J. Hu, Y.-C. Han, and S.-L. Cong, *Phys. Rev. A* **94**, 032705 (2016).
- [46] T. Kraemer, M. Mark, P. Waldburger, J. G. Danzl, C. Chin, B. Engeser, A. D. Lange, K. Pilch, A. Jaakkola, H.-C. Nägerl and R. Grimm, *Nature* **440**, 315 (2006).
- [47] F. Ferlaino, A. Zenesini, M. Berninger, B. Huang, H.-C. Nägerl, and R. Grimm, *Few-Body Syst.* **51**, 113 (2011).
- [48] S. E. Pollack, D. Dries, and R. G. Hulet, *Science* **326**, 1683 (2009).
- [49] P. Dyke, S. E. Pollack, and R. G. Hulet, *Phys. Rev. A* **88**, 023625 (2013).
- [50] N. Gross, Z. Shotan, S. Kokkelmans, and L. Khaykovich, *Phys. Rev. Lett.* **103**, 163202 (2009).
- [51] N. Gross, Z. Shotan, O. Machtey, S. Kokkelmans, and L. Khaykovich, *Comp. Rend. Phys.* **12**, 4 (2011).
- [52] N. Gross, Z. Shotan, S. Kokkelmans, and L. Khaykovich, *Phys. Rev. Lett.* **105**, 103203 (2010).
- [53] M. Zaccanti, B. Deissler, C. D'Errico, M. Fattori, M. Jona-Lasinio, S. Müller, G. Roati, M. Inguscio, and G. Modugno, *Nat. Phys.* **5**, 586 (2009).
- [54] S. Knoop, F. Ferlaino, M. Mark, M. Berninger, H. Schöbel, H.-C. Nägerl, and R. Grimm, *Nat. Phys.* **5**, 227 (2009).
- [55] A. Zenesini, B. Huang, M. Berninger, H.-C. Nägerl, F. Ferlaino, and R. Grimm, *Phys. Rev. A* **90**, 022704 (2014).
- [56] O. Machtey, Z. Shotan, N. Gross, and L. Khaykovich, *Phys. Rev. Lett.* **108**, 210406 (2012).
- [57] T. Lompe, T. B. Ottenstein, F. Serwane, K. Viering, A. N. Wenz, G. Zürn, and S. Jochim, *Phys. Rev. Lett.* **105**, 103201 (2010).
- [58] S. Roy, M. Landini, A. Trenkwalder, G. Semeghini, G. Spagnolli, A. Simoni, M. Fattori, M. Inguscio, and G. Modugno, *Phys. Rev. Lett.* **111**, 053202 (2013).
- [59] O. Machtey, D. A. Kessler, and L. Khaykovich, *Phys. Rev. Lett.* **108**, 130403 (2012).
- [60] C. Langmack, D. H. Smith, and E. Braaten, *Phys. Rev. A* **86**, 022718 (2012).
- [61] M.-G. Hu, R. S. Bloom, D. S. Jin, and J.M. Goldwin, *Phys. Rev. A* **90**, 013619 (2014).
- [62] V. V. Flambaum, G. F. Gribakin, and C. Harabati, *Phys. Rev. A* **59**, 1998 (1999).
- [63] Y. Wang and P. S. Julienne, *Nat. Phys.* **10**, 768 (2014).
- [64] B. Huang, L. A. Sidorenkov, R. Grimm, and J. M. Hutson, *Phys. Rev. Lett.* **112**, 190401 (2014).
- [65] P. Giannakeas and C. H. Greene, arXiv:1608.08276 (2016).